THE JOURNAL OF PHYSICAL CHEMISTRY C

Article

pubs.acs.org/JPCC

Scattering of Atomic Hydrogen Off a H-Covered W(110) Surface: Hot-Atom versus Eley–Rideal Abstraction Dynamics

R. Pétuya,[†,‡] P. Larrégaray,*[,†,‡] C. Crespos,[†,‡] P. Aurel,[†,‡] H. F. Busnengo,[§] and A. E. Martínez[§]

[†]ISM, CNRS UMR 5255, Université de Bordeaux, 33405 Talence Cedex, France

[‡]ISM, UMR5255, CNRS, F-33400 Talence, France

[§]Instituto de Física Rosario (IFIR) CONICET-UNR, Esmeralda y Ocampo, 2000 Rosario, Argentina

ABSTRACT: Normal incidence scattering of hydrogen atoms off a H-covered tungsten W(110) surface is simulated via quasiclassical trajectories. A density functional theory (DFT) based multiadsorbate potential is developed to model a wide range of surface coverages, θ = 0.25–1 monolayer (ML), reproducing the surface arrangements observed at low temperature. The competition between hot-atom (HA) and Eley–Rideal (ER) abstraction mechanisms is studied for collision energies of the projectile atom in the range E_p = 0.1–5.0 eV (E_p = 0.1–2.0 eV) for θ = 0.25 ML (θ = 0.5, 0.75, and 1 ML) coverage. Cross sections, final energies of the recombination products, and reaction times are analyzed. At low coverage and low collision energy, HA dominates the abstraction, whereas HA and ER cross-sections become similar when collision energy increases. The vibrational distribution of recombined H_2 molecules at finite coverage is found to be in better agreement with experiments than the one computed within the single adsorbate limit. At high surface coverage, ER dominates abstraction but the dynamical observables highlight the similarity between both reaction mechanisms, thus suggesting that abstraction may be considered as a unique process.

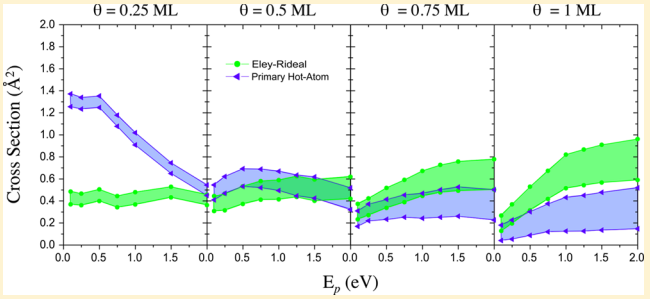

1. INTRODUCTION

Over the last 20 years, many studies have addressed the Eley–Rideal (ER) and hot-atom (HA) reactions of hydrogen molecules on metal surfaces experimentally[1−14] and theoretically.[15−33] At low surface temperatures, Langmuir–Hinshelwood[34] reactivity for hydrogen recombination on most metals is expected to be small as the process is usually significantly endothermic. Recombination is consequently governed by ER or HA abstraction[35] in the presence of gas-phase atomic species. In the ER abstraction, an atom impinging from the gas phase (projectile) recombines directly with an adsorbate (target) in a single collision with the surface. In the HA reaction, the projectile diffuses on the surface before recombination. During this diffusion step, initially at hyperthermal energy, the projectile experiences several encounters with the surface and can exchange energy, before recombination, with the surface or the adsorbates at finite coverage. However, as far as hydrogen is concerned, because of mass ratio, the incident atom is expected to mainly lose energy through collisions with adsorbates and dissipation to phonons is thought to be negligible.[21,22,36] Nevertheless, electron–hole pair[37] excitations might also play a non-negligible role. Comparison between experimental[1,3] and theoretical studies for recombination of H(D) atoms with D(H)-covered Cu(111) surface[19,20,22,38,39] have suggested that HA dominates the reaction: the experimental total abstraction cross sections were found 1 order of magnitude greater than ER theoretical cross sections computed within the single adsorbate limit. Pioneering theoretical dynamics studies taking into account surface coverage[21,22,25,28,40−42] have led to a better agreement with the kinetic experiments at low collision energies (<0.3 eV).

The recombination of hydrogen on tungsten is of special interest, as this metal is the main candidate for the divertors of the ITER fusion reactor.[43−47] However, theoretical works[15−18,32,48,49] on this process were only performed in the single adsorbate limit and thus restricted to the description of the ER process. H-covered W(110) surfaces have also generated fundamental interest because of the substrate phonon anomalies observed near saturation coverage and specific surface arrangements of adsorbates at low temperature (<250 K) and lower coverages (θ = 0.5 and 0.75 monolayer (ML)).[50−59]

In this paper, the competition between the HA and ER processes, for the H+H/W(110) system, is investigated via quasi-classical trajectory (QCT) simulations under normal incidence. We first present a multiadsorbate PES developed following the original idea by Shalashilin and Jackson (S&J).[21,22] This PES, based on density-functional-theory (DFT) calculations and interpolated using the corrugation reducing procedure (CRP),[60] predicts equilibrium structures for the H-covered tungsten surface in reasonable agreement with observed surface arrangements, for the coverages studied

Received: November 27, 2014
Revised: January 14, 2015
Published: January 15, 2015

DOI: 10.1021/jp511847w
J. Phys. Chem. C 2015, 119, 3171−3179

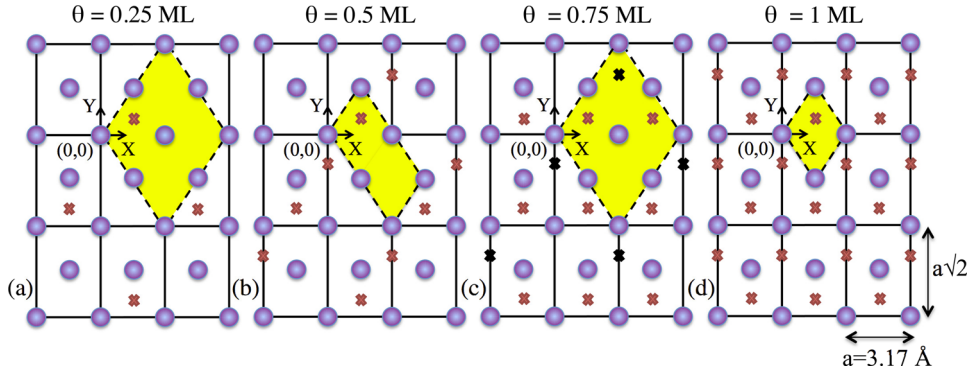

Figure 1. Positions of the adsorbed H atoms at (a) θ = 0.25 ML, (b) θ = 0.5 ML, (c) θ = 0.75 ML, and (d) θ = 1 ML. The crosses represent the H atoms positions and a = 3.17 Å is the lattice constant parameter. On (c), red and black crosses are used to differentiate the two sublattices for θ = 0.75 ML. Sampling areas of initial (X_p, Y_p) positions of the projectiles for each coverage are represented in yellow.

in this work. Dynamics simulations are then performed for θ = 0.25 ML coverage, focusing on the effect of collision energy and the distinction between both abstraction mechanisms from dynamical observables such as final energies, reaction times, or angular distributions of the produced H_2 molecules. The influence of the surface coverage on the HA vs ER competition is then investigated for θ = 0.5, 0.75, and 1 ML. Comparison with available experimental data is also presented.

The paper is structured as follow. Characteristics of the multiadsorbate PES and methodological details of the QCT simulations are presented in section 2. In section 3, results from the dynamics are described and discussed. Section 4 concludes.

2. THEORY

Multiadsorbate PES. In a recent work,[48] we have extended the CRP PES, developed by Busnengo et al.[61] for the investigation of H_2 chemisorption on W(110), to the study of ER abstraction dynamics. In this interpolation scheme, the full 6-dimension (6D) PES, V^{6D}, is decomposed as sum of the atom-surface 3-dimension potentials, V^{3D}, and a remaining 6D interpolation function, I^{6D}:

$$V^{6D}(\mathbf{r}_1,\mathbf{r}_2) = V^{3D}(\mathbf{r}_1) + V^{3D}(\mathbf{r}_2) + I^{6D}(\mathbf{r}_1,\mathbf{r}_2) \quad (1)$$

where $\mathbf{r}_1$ and $\mathbf{r}_2$ are the position vectors of both atoms. Within a good approximation $I^{6D}(\mathbf{r}_1,\mathbf{r}_2) = 0$ when the interatomic distance $r = \|\mathbf{r}_1 - \mathbf{r}_2\| \geq 3.0$ Å. To describe the interaction of the tungsten surface with more than two atoms and account for finite surface coverage, we here adapt, to the CRP PES, the idea first developed by S&J[21,22] which consists in expanding the multiadsorbate potential $V(\{\mathbf{r}_i\})$ as a two-body terms sum for the N H atoms:

$$V(\{\mathbf{r}_i\}) = \sum_{i=1}^{N} V^{3D}(\mathbf{r}_i) + \sum_{i=1}^{N}\sum_{j>i}^{N} I^{6D}[\mathbf{r}_i,\mathbf{r}_j] \quad (2)$$

where $\mathbf{r}_i$ is the position vector of atom i. The underlying assumption is that three H atom interactions are negligible during the dynamics. Such a limitation is discussed in the next subsection.

In agreement with experiments[50,54−56] and previous DFT calculations,[59,61,62] the most stable atomic adsorption site predicted by the interpolated PES is located very close to the 3-fold hollow site (X = 1.585 Å, Y = 0.6503 Å, and Z = 1.07 Å in the primitive cell), with a chemisorption energy of 3.06 eV. For θ = 0.25 ML, the targets are adsorbed in such a position (Figure 1a) and distributed on the surface to maximize the distance between adsorbates. However, with increasing coverage, interactions between adsorbates slightly modify the equilibrium positions. Exact equilibrium positions on the PES, for each coverage, are displayed in Table 1. Despite the high mobility of the H atoms at low coverage, when including zero point energy (see next section), the multiadsorbate PES is able to reproduce the observed surface arrangements at low temperature.[50−55] Ordered p(2×1) and (2×2) configurations are characterized for θ = 0.5 ML (Figure 1b) and θ = 0.75 ML (Figure 1c), respectively, which disorder around 200 K in the former case and 250 K in the latter one.[51−53] At θ = 0.75 ML, in agreement with experiment, the PES shows two sublattices of adsorbates differentiated by red and black crosses in Figure 1c. The adsorbates on the black crosses are surrounded by four nearest neighbors whereas the adsorbates on the red crosses have two nearest and two next-nearest neighbors. Accordingly, they adopt slightly different equilibrium positions (Table 1). Close to saturation, coverage θ = 1 ML, the H atoms follow a (1×1) structure (Figure 1d) and exhibit a great mobility around their adsorption site but still stay in their original unit cell conserving

Table 1. Equilibrium Positions of the Adsorbates (for Adsorbates in the Origin Cell) for the Multiadsorbate PES and DFT Calculations[a]

coverage		multiadsorbate PES (Å)	DFT (Å)	ΔE (meV)	ZPE (meV)
θ = 0.25	X	1.585	1.585	0.66	47
	Y	0.6503	0.6478		60
	Z	1.07	1.08		71
θ = 0.5	X	1.585	1.573	11.8	34
	Y	0.6803	0.684		48
	Z	1.15	1.116		78
θ = 0.75	X	1.591	1.571	34.9	35
red crosses	Y	0.6823	0.6725		47
Figure 1	Z	1.145	1.124		76
θ = 0.75	X	1.585	1.5849		40
black crosses	Y	0.6923	0.6969		54
Figure 1	Z	1.216	1.135		82
θ = 1.0	X	1.585	1.585	80.6	41
	Y	0.6993	0.6825		50
	Z	1.1974	1.1207		81

[a] ΔE represents the total DFT energy difference between the multiadsorbate PES and DFT equilibrium positions. Values for the assigned ZPE, for each vibrational mode (X, Y, and Z), are displayed in the last column.[55]

DOI: 10.1021/jp511847w
J. Phys. Chem. C 2015, 119, 3171−3179

the (1×1) structure qualified as a "two-dimensional quasi-liquid-like phase" by Balden et al.[55] To check the accuracy of the multiadsorbate PES, regarding these surface arrangements, we performed DFT optimizations using the parameters previously used for the construction of the CRP PES.[61] The primitive cell for the DFT calculation is displayed in yellow in Figure 1. At each surface coverage, the agreement between the multiadsorbate PES and DFT equilibrium positions is reasonable and discrepancies in total DFT energy (ΔE) between both structures are small (Table 1). The major differences in the equilibrium positions appear in the normal coordinate (Z) for which the multiadsorbate PES leads to higher relaxation. Nevertheless, the two sublattices of adsorbates at θ = 0.75 ML are also revealed by the DFT calculations.

Dynamics. The normal incidence scattering of an H projectile over an H-covered W(110) surface is simulated via QCT for θ = 0.25, 0.5, 0.75, and 1 ML. Within the Born−Oppenheimer approximation, the dynamics simulations are performed on the ground state PES. The surface is considered static and coupling with phonons is not included. Due to the large mass mismatch, energy dissipation to phonons is expected to be slow in comparison with the simulation time scale. Conversely, collisions with H adsorbates are expected to lead to the dominant energy-transfer mechanism.[21,22,36] Electron−hole pair excitations, which have been recently suggested as a significant energy loss channel for hydrogen atoms hyperthermal diffusion on Pd(100),[37] are here neglected. This may affect quantitatively the results of the present work, in particular for the HA process at low coverage.

To model an infinite covered surface, a 6 × 6 rectangular ($a \times a\sqrt{2}$) array with periodic boundaries conditions was used. The classical equations of motion were numerically integrated with a Beeman algorithm[63,64] for 18, 36, 54, and 72 targets for respectively θ = 0.25, 0.5, 0.75, and 1 ML. We increased the simulation cell size up to a 12 × 12 (10 × 10) array with 72 (100) targets at θ = 0.25 ML (θ = 0.5 ML). In agreement with previous works,[21,22,25,28,40−42] changes on the results were not significant. Initial conditions for the QCT simulations were the following: the targets sit in their equilibrium positions (Table 1 and Figure 1) and are given an initial ZPE. For θ = 0.25 ML, the targets initially do not interact between themselves (I^{6D} = 0); therefore, the ZPE (Table 1) were calculated in the single adsorbate limit through a X, Y, and Z mode decomposition.[48,49] For higher coverages, the experimental ZPE values (Table 1) were used.[55] We checked that a change by a factor 2 in the value of the ZPE does not affect the results of the dynamics. The H projectile starts in the asymptotic region of the potential, i.e., at 7.0 Å from the surface. Its (X_p, Y_p) initial coordinates are randomly sampled in the primitive cell of the H-covered surface, displayed for each coverage in yellow in Figure 1. For each collision energy, we compute 120 000 trajectories for θ = 0.25 ML and θ = 0.75 ML, 60 000 trajectories for θ = 0.5 ML and 30 000 trajectories for θ = 1 ML.

Integration of the trajectories is performed until one atom enters the surface below Z = −0.75 Å (*absorption*), one atom (*reflection*) or one molecule (*abstraction*) reaches the initial altitude of the projectile, or the total integration time of 2 ps is completed (*adsorption*). As shown in the following section, the total integration time is sufficient to allow all processes to happen. Among the *total abstraction* channel, *Eley−Rideal* abstraction occurs when projectile and target recombine with only one rebound of the center of mass of the molecule after the collision between projectile and surface. Otherwise the abstraction is counted as *primary hot-atom*. Whether the abstraction takes place involving two targets, it is classified as a *secondary hot-atom*. The cross section per adsorbate for each mechanism is defined by

$$\sigma = \int\int_D \frac{P(X_p,Y_p)}{N_t} dX_p\, dY_p \tag{3}$$

with integration over D, the sampling area in yellow in Figure 1. $P(X_p,Y_p)$, the two-dimensional opacity function, is the probability of each mechanism for a given set of initial coordinates (X_p, Y_p) of the projectile and N_t is the number of targets initially adsorbed in the sampling area. A Gaussian weighting binning[65−67] procedure is applied to semiclassically quantize the final vibration of the H_2 diatom. In such a procedure, each trajectory is weighted by a Gaussian coefficient depending on the value of the final (real) vibrational action with respect to the nearest entire one (semiclassical counterpart of the vibration quantum number). This procedure was found to significantly improve the QCT prediction of state distributions in the quantum regime, i.e., when few vibrational levels are available to the products. This is typically the case when significant energy dissipation to the adsorbates occurs during hot-atom abstraction.

As mentioned earlier, the PES is limited to a two-adsorbate terms expansion and can lead to unphysical results when three H atoms are too close. Therefore, trajectories are stopped when one H atom has two other H atoms closer than 1.5 Å (twice the equilibrium distance in vacuum). The actual fate of these trajectories is thus unknown. At θ = 0.25 ML coverage, the simulations describe correctly over the E_p = 0.1−5.0 eV energy range, at least 92.5% of the total reactive trajectories. At this coverage, we represent the total cross section of stopped trajectories as error bars for each exit channel. With increasing the coverage, the proportion of stopped trajectories increases and we had to limit the energy range studied to E_p = 0.1−2.0 eV. In this energy range the simulations model correctly at least 84.6% of the total reactive trajectories at θ = 0.5 ML, 76.8% at θ = 0.75 ML, and 67.1% at θ = 1 ML. We thus predict a range of possible cross sections by assuming that either 0% or 100% of the stopped trajectories lead to ER and primary HA channels. Though quantitative analysis at high coverage should be regarded with caution, this makes possible a qualitative analysis of the ER vs HA competition.

3. RESULTS AND DISCUSSION

Coverage θ = 0.25 ML. The cross sections for the different above-defined outcomes of the scattering are displayed in Figure 2 as a function of the perpendicular initial energy of the projectile, E_p, at θ = 0.25 ML coverage. At very low collision energy, most of the projectiles adsorb on the surface. As E_p increases, the adsorption cross section rapidly decreases at the expense of absorption and reflection channels. The total abstraction cross section, which is found 1 order of magnitude lower than the sum of the other channels, similarly decreases over the 0.1−5.0 eV energy range. At low energy, the primary HA process is found much higher (almost 4 times) than ER, as observed in previous studies (lower panel of Figure 2.).[21,22,25] However, when E_p increases, the HA abstraction decreases rapidly whereas ER abstraction remains almost constant until E_p = 2.0 eV. These two processes thus lead to similar cross

DOI: 10.1021/jp511847w
J. Phys. Chem. C 2015, 119, 3171−3179

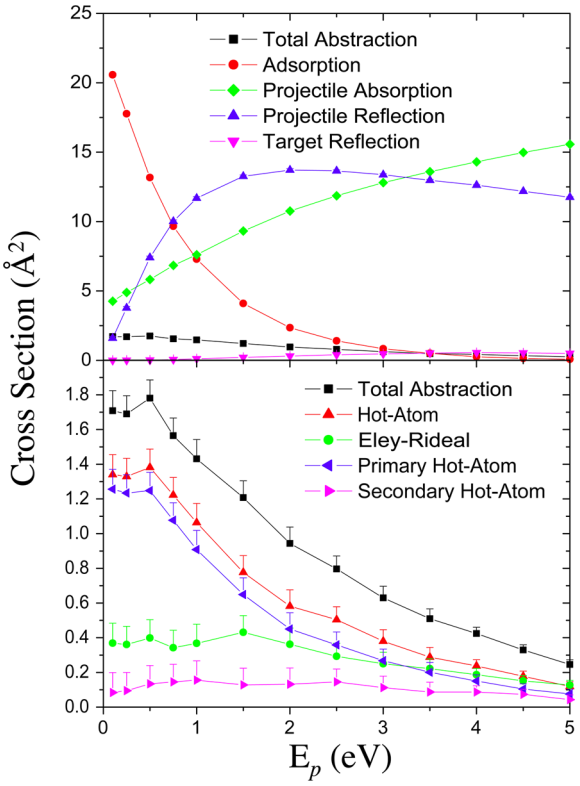

Figure 2. Cross sections (Å^2) as a function of the initial energy of the projectile E_p (eV) at θ = 0.25 ML. Upper panel presents the main exit channels whereas lower panel details the abstraction mechanisms.

sections for energies higher than 2.5 eV. Because of a different sampling area of the initial (X_p, Y_p) positions of the projectiles and recombination with targets initially adsorbed outside the sampling area, ER cross section is slightly higher than the one computed within the single adsorbate limit.[48,49] Consistently with previous works[48,49,68,69] such ER trajectories bounce on a W surface atom prior to recombination. The secondary HA contribution to the abstraction cross section remains low and constant (~0.1 Å^2).

In Figure 3, the final average translational, rotational, and vibrational energy of the recombined molecules are represented as a function of E_p. As already observed in single adsorbate studies,[48,49] most of the available energy is transferred to translational motion. Both ER and HA processes produce rotationally and vibrationally excited molecules. Nevertheless, molecules formed via ER abstraction appear to be more excited than the ones recombined via primary HA mechanism. The HA, diffusing close to the surface (Figure 3), might scatter from other adsorbates, thus transferring energy before recombination. A secondary HA mechanism requires a sufficient energy transfer from the projectile to one adsorbate to kick it out of its adsorption site before the latter recombines with another target. Thus, as observed in Figure 3, final energies of this channel are much lower than others. For θ = 0.25 ML, ER abstraction total final energy and partition between the different degrees of freedom are identical to results obtained within the single adsorbate limit.[48]

Figure 4 displays the final time distributions of the different reactive channels for E_p = 1.0 eV. At this collision energy and coverage, ER abstraction appears to be faster than 0.25 ps whereas most of primary HA abstraction happens between 0.25 and 0.75 ps. We also display the distributions of exit polar angle

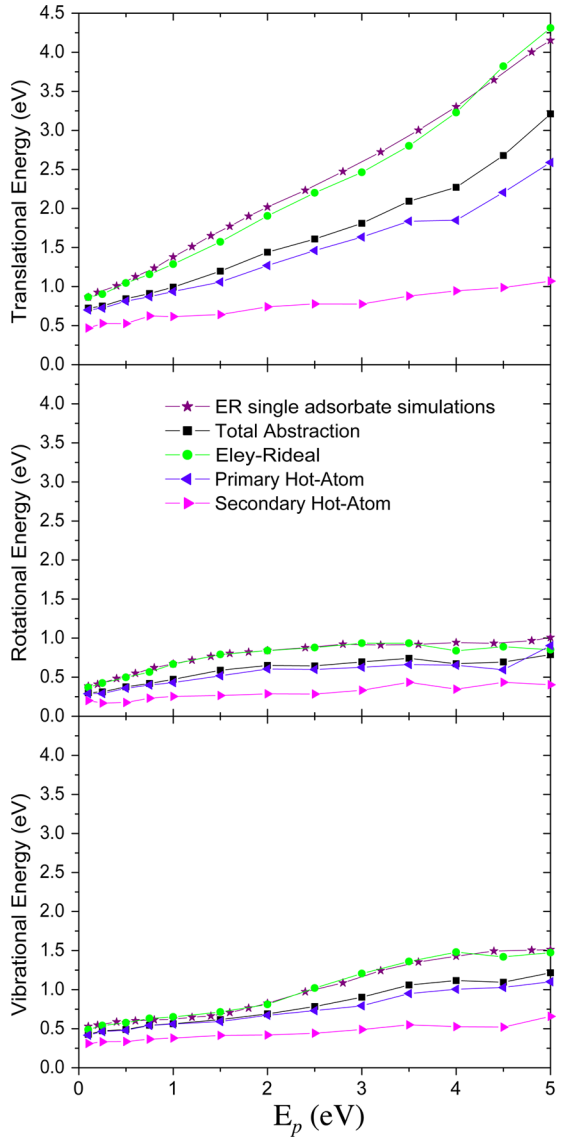

Figure 3. Final average translational (upper panel), rotational (middle), and vibrational (lower panel) energies plotted as a function of the initial energy of the projectile, E_p (eV) at θ = 0.25 ML. The results from ER abstraction within the single adsorbate limit are displayed as purple stars.[48]

Θ_E of the produced molecules (respect to the surface normal axis) divided by sin Θ_E. ER and primary HA processes do not lead to distinct signatures on the contrary to recombination on Cu(111),[22] for which H_2 molecules leave the surface close to the normal direction.

Influence of the Coverage. We now investigate the influence of surface coverage on the dynamics. In Figure 5, the possible range for ER and primary HA cross sections are represented for coverages θ = 0.25, 0.5, 0.75, and 1 ML as a function of the perpendicular initial energy of the projectile in the range E_p = 0.1−2.0 eV. With increasing coverage, important changes on the cross sections can be noticed. At low coverage, θ = 0.25 ML (Figure 2), the primary HA cross section is a maximum at very low collision energy and decreases with increasing E_p whereas at higher coverage it starts from much lower values and increases up to E_p = 0.5 eV (E_p = 1.5 and 2.0 eV) for θ = 0.5 ML (θ = 0.75 and 1 ML). This coverage-dependent diminution at low collision energy results from an

DOI: 10.1021/jp511847w
J. Phys. Chem. C 2015, 119, 3171−3179

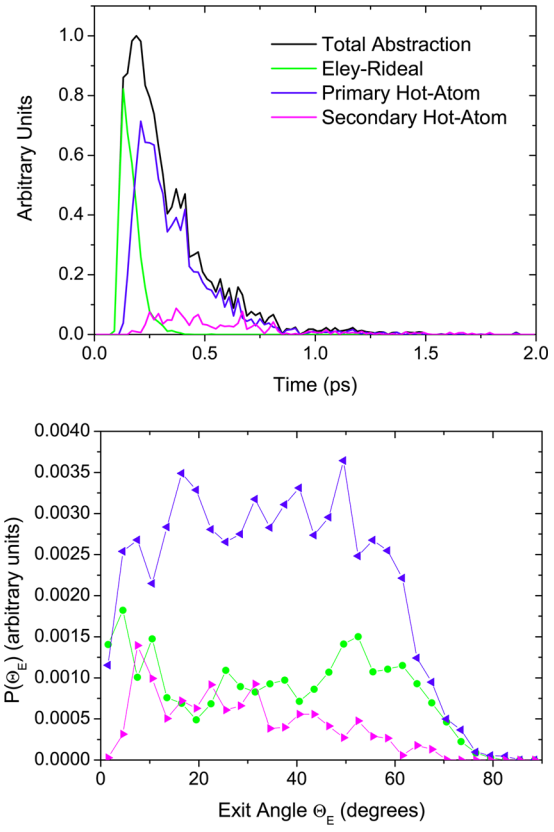

Figure 4. Final time distributions of abstraction for E_p = 1.0 eV (upper panel). Distributions of exit polar angles Θ_E of the formed molecules (lower panel), with respect to the surface normal axis. On the lower panel, the color code is the same than Figure 2 and 4 240 000 trajectories have been computed for these plots.

increase of the adsorption channel which is found to be more probable than absorption and reflection of the projectile even when the collision energy increases (not shown). At θ = 0.5 ML, the ER cross section does not change much from θ = 0.25 ML but ER and primary HA cross sections are comparable. With increasing coverage, the ER mechanism clearly raises up and dominates the molecular hydrogen formation and cannot be disregarded as in low coverage and low energy studies.[21,22]

Figure 6 displays the total abstraction time distributions at E_p = 1.0 eV for the four coverages studied in this work. In

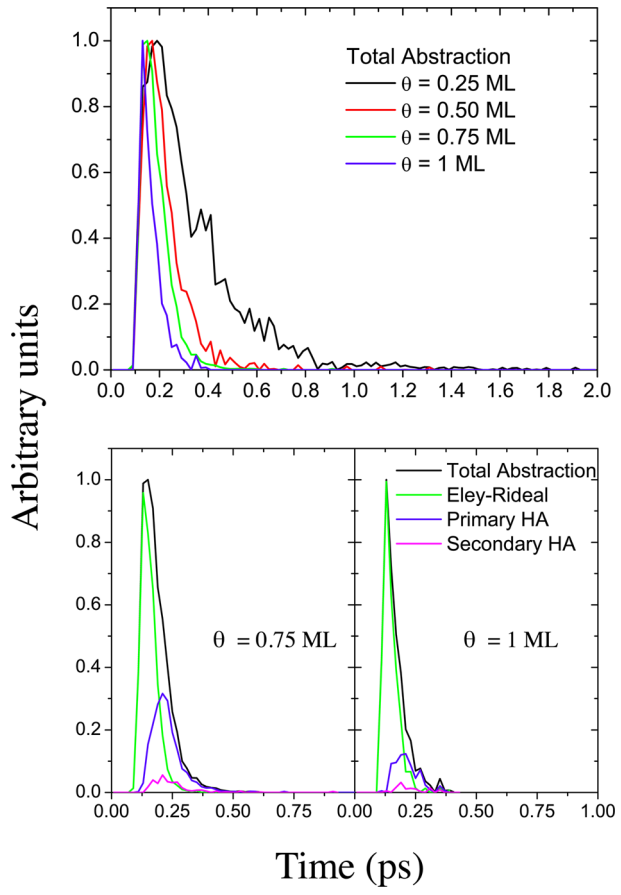

Figure 6. Upper panel: total abstraction time distributions for E_p = 1.0 eV at the different coverages studied. Lower panel: times distributions of abstraction mechanisms for E_p = 1.0 eV at θ = 0.75 ML (left) and θ = 1 ML (right).

agreement with a previous work,[25] we observe that lowering the coverage consistently increases the abstraction time. In the lower panel, we detail the time distributions for the abstraction mechanism at θ = 0.75 ML (left) and θ = 1 ML (right). Comparison with Figure 4 highlights the increasing contribu-

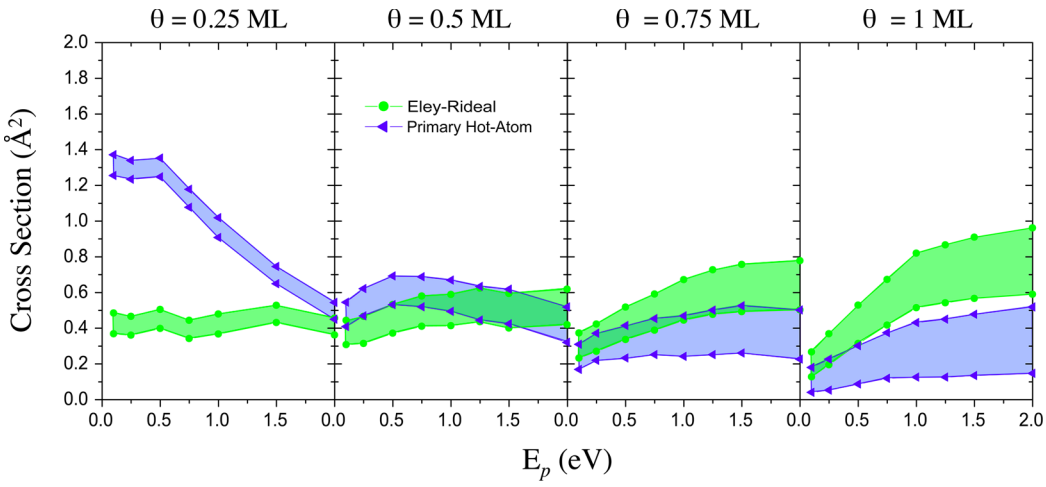

Figure 5. Cross sections (Å^2) as a function of the initial energy of the projectile E_p (eV) for different coverages.

DOI: 10.1021/jp511847w
J. Phys. Chem. C 2015, 119, 3171−3179

tion of ER with increasing coverage. Moreover, both primary and secondary HA take place on the same time scale as ER at θ = 1 ML.

In Figure 7, the final average translational, rotational, and vibrational energies of the recombined molecules at θ = 0.5, 0.75, and 1 ML (to be compared with Figure 3) are displayed. The diatom final energies, when accounting for all abstraction channels, are not much affected by coverage changes. However, final energies for diatoms resulting from ER recombination are much lower than that from the single adsorbate limit,[48] but still more excited than the ones corresponding to HA abstraction. At θ = 0.5 ML coverage, the final average total energy of ER trajectories represents on average 85% of the value at θ = 0.25 ML, the remaining part being transferred to other adsorbed atoms. This proportion decreases to 77% and 68% with increasing coverage respectively to θ = 0.75 and 1 ML. In the single adsorbate limit and at θ = 0.25 ML coverage, ER abstraction proceed via collision with a W surface atom prior to recombination, which role is to redirect the projectile toward the target. When surface coverage increases, the projectile is more likely to scatter from a target and transfer some energy in its way to another adsorbate with which it recombines.

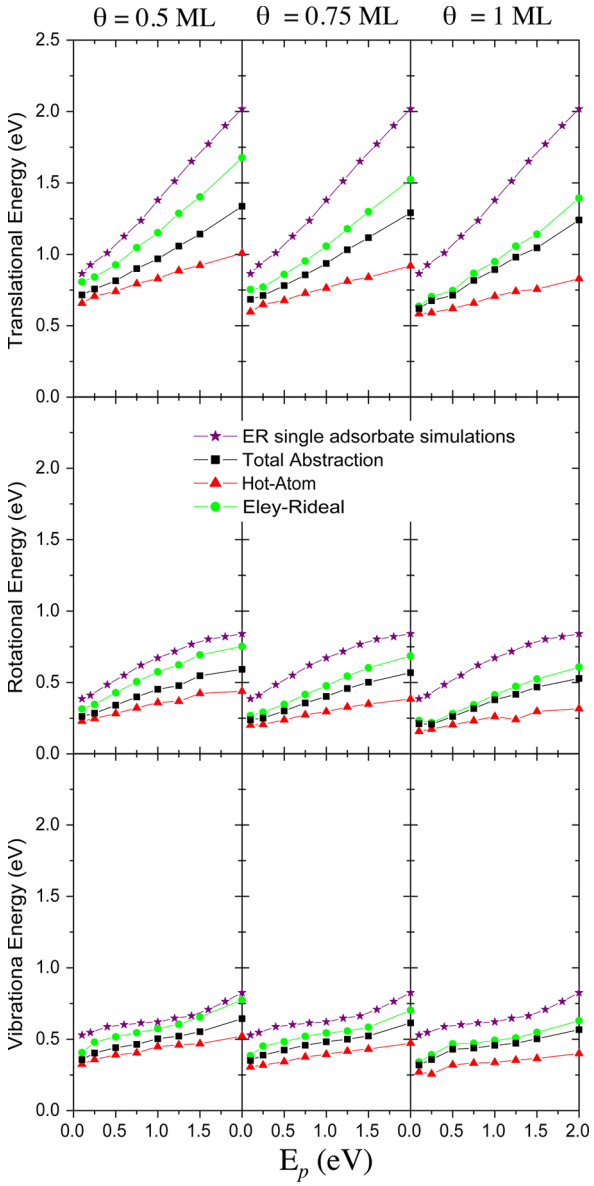

Figure 7. Final average translational (upper panel), rotational (middle), and vibrational (lower panel) energies represented as a function of the initial energy of the projectile, E_p, at coverages θ = 0.5 (left), 0.75 (middle), and 1 ML (right). Purple stars represent the results obtained for the ER abstraction studies in the single adsorbate limit.[48]

In the following section, we compare the vibrational populations simulated with experiments performed at 2000 K. Figure 8 displays the vibrational distributions for collision energies E_p = 0.1 and 0.25 eV, which are about the average collision energy of the experiments. In this energy range, vibrational populations are not much affected by coverage changes between θ = 0.25 and 0.75 ML. Therefore, in the following section, the comparison with experiments, for which coverage is unknown, should not be drastically affected by such coverage changes.

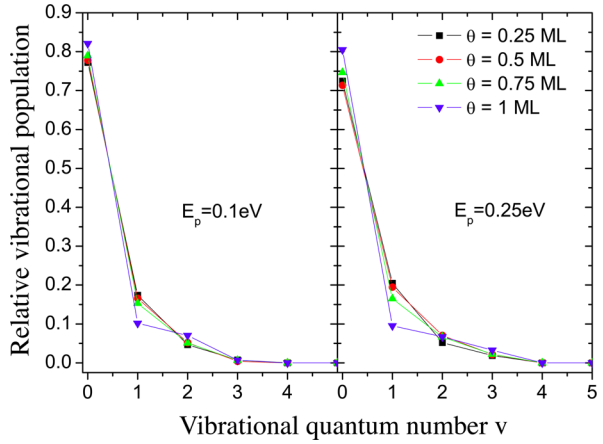

Figure 8. Relative vibrational populations of the recombined molecules for the different coverage studied at collision energy E_p = 0.1 (left) and 0.25 eV (right).

The influence of surface coverage on the dynamics highlights the difficulty to differentiate ER and primary HA processes at high coverage. The balance between both mechanisms changes. ER is not negligible anymore and shares many characteristics with the primary HA process. Both abstraction processes occur on the same time scale and both experience collision and energy exchange with adsorbate before recombination. These observations suggest that at high coverage ER and primary HA are hardly separable. The distinction between both is thus somewhat arbitrary.

Comparison with Experiments. Experiments of molecular hydrogen recombination on polycrystalline tungsten samples have recently been performed by Markelj et al.[70] In this experiment, hydrogen atoms are previously dissociated on a tungsten filament at 2000 K. In a recent work, we compared the results of the simulations of ER abstraction with such experiments. To that end, a thermal averaging of the simulated vibrational population detailed in refs 48 and 71 was performed. As apparent from Figure 9, such simulations lead to vibrational distributions slightly to hot, though qualitatively correct. Besides, in previous studies,[28,49] vibrational excitation has been found weakly dependent on surface symmetry and surface temperature. Therefore, we compute vibrational populations in the static surface approximation at θ = 0.25 ML and perform a

DOI: 10.1021/jp511847w
J. Phys. Chem. C 2015, 119, 3171−3179

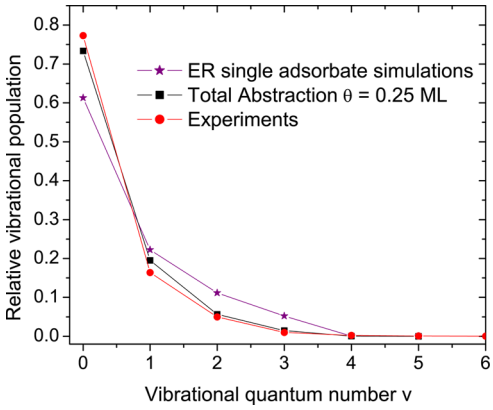

Figure 9. Relative vibrational populations of the recombined molecules. Purple stars represent the ER single adsorbate limit[48] at a surface temperature of 300 K, and black squares represent the total abstraction results at θ = 0.25 ML in the static surface approximation. Experimental results are in red dots. Lines are drawn to guide the eye. Experimental results for excitation higher than v = 6 (population about 10^{-4} and lower) are not represented.

thermal averaging of the vibrational populations[48,71] to compare with experimental data. As both normal and total energy scaling limits give similar results, we only consider the normal energy scaling limit.

Figure 9 displays the vibrational distributions for the total abstraction channel at θ = 0.25 ML and for ER recombination within the single adsorbate limit.[48] Results taking into account the HA processes are in much better agreement with experiments for levels v = 0 to v = 3. Populations of higher levels are almost negligible. ER and HA processes cannot be discrimiated in these experiments and the results provide evidence for the necessity to simulate all the abstraction mechanisms to obtain a correct description of the product vibrational excitation.

4. CONCLUSION

QCT simulations of atomic hydrogen normal incidence scattering over an H-covered W(110) surface are presented for θ = 0.25, 0.5, 0.75, and 1 ML coverages within the static surface approximation. A multiadsorbate PES is developed as a sum of CRP atom-surface potentials and a two-body term expansion of atom−atom interpolation functions. In agreement with previous works, the HA process dominates the abstraction of H_2 at low coverage (θ = 0.25 ML) and low collision energy. The abstraction time scale is subpicosecond. ER and HA processes produce vibrationally and rotationally hot molecules; however, ER leads to the more excited ones. Vibrational distributions of the recombined molecules for finite coverage are found in better agreement with experiments than the one computed within the single adsorbate limit. With increasing surface coverage, HA versus ER balance changes to make ER an equivalent (θ = 0.5 ML) or dominant (θ = 0.75, 1 ML) channel. Moreover, the total abstraction time decreases and both primary HA and ER processes take place on a similar time scale at saturation coverage. The partition of average energy between translation, rotation, and vibration is weakly affected by coverage changes. However, ER average final energies decrease when the surface coverage increases because of scattering of other adsorbates before recombination. At high surface coverage, ER and primary HA dynamics share lots of similarities, thus highlighting the arbitrary character of their separation. Primary recombination at high coverage should be considered as a unique reactive process.

AUTHOR INFORMATION

Corresponding Author

*P. Larrégaray. E-mail: pascal.larregaray@u-bordeaux.fr. Tel: +33540002961.

Notes

The authors declare no competing financial interest.

ACKNOWLEDGMENTS

The authors acknowledge the support of France Grilles for providing computing resources on the French National Grid Infrastructure and ECOS-sud program for funding. AEM and HFB also acknowledge financial support from CONICET (project PIP 0667), ANPCyT (project PICT Bicentenario No. 1962), and UNR (project PID ING404).

REFERENCES

(1) Rettner, C. T. Dynamics of the direct reaction of hydrogen atoms adsorbed on Cu(111) with hydrogen atoms incident from the gas phase. *Phys. Rev. Lett.* **1992**, *69*, 383−386.
(2) Rettner, C. T. Reaction of an H-atom beam with Cl/Au(111): Dynamics of concurrent Eley-Rideal and Langmuir−Hinshelwood mechanisms. *J. Chem. Phys.* **1994**, *101*, 1529−1546.
(3) Rettner, C. T.; Auerbach, D. J. Dynamics of the Eley-Rideal Reaction of D Atoms with H Atoms Adsorbed on Cu(111): Vibrational and Rotational State Distributions of the HD Product. *Phys. Rev. Lett.* **1995**, *74*, 4551−4554.
(4) Kim, J. Y.; Lee, J. Spatial and Kinetic Separation of Eley-Rideal Plus Primary Hot Atom and Secondary Hot Atom Mechanisms in H Atom Abstraction of Adsorbed D Atoms on Pt(111). *Phys. Rew. Lett.* **1999**, *82*.
(5) Kim, J. Y.; Lee, J. Kinetics, mechanism, and dynamics of the gas-phase H(D) atom reaction with adsorbed D(H) atom on Pt(111). *J. Chem. Phys.* **2000**, *113*, 2856−2865.
(6) Kammler, T.; Wehner, S.; Küppers, J. Interaction of thermal H atoms with Ni(100)-H surfaces: through surface penetration and adsorbed hydrogen abstraction. *Surf. Sci.* **1995**, *339*, 125−134.
(7) Kammler, T.; Lee, J.; Küppers, J. A kinetic study of the interaction of gaseous H(D) atoms with D(H) adsorbed on Ni(100) surfaces. *J. Chem. Phys.* **1997**, *106*, 7362−7371.
(8) Zecho, T.; Brandner, B.; Küppers, J. Abstraction of D adsorbed on Pt(100) surfaces by gaseous H atoms: effect of surface heterogeneity. *Surf. Sci. Lett.* **1998**, *418*, L26−L30.
(9) Wehner, S.; Küppers, J. Abstraction of H adsorbed on Pt(111) surfaces with gaseous D atoms: isotope and flux effects. *Surf. Sci.* **1998**, *411*, 46−53.
(10) Wehner, S.; Küppers, J. Interaction of gaseous D atoms with CH_3I adsorbed on Pt(111), H/Pt(111), and C/Pt(111) surfaces: From hot-atom to Eley−Rideal phenomenology. *J. Chem. Phys.* **1998**, *109*, 294−300.
(11) Wehner, S.; Küppers, J. Abstraction of D adsorbed on Pt(111) surfaces with gaseous H atoms. *J. Chem. Phys.* **1998**, *108*, 3353−3359.
(12) Kammler, T.; Wehner, S.; Küppers, J. The role of sticking and reaction probabilities in hot-atom mediated abstraction reactions of D on metal surfaces by gaseous H atoms. *J. Chem. Phys.* **1998**, *109*, 4071−4077.
(13) Kammler, T.; Küppers, J. Interaction of H atoms with Cu(111) surfaces: Adsorption, absorption, and abstraction. *J. Chem. Phys.* **1999**, *111*, 8115−8123.
(14) Kolovos-Vellianitis, D.; Kammler, T.; Küppers, J. Interaction of gaseous H atoms with Cu(100) surfaces: adsorption, absorption, and abstraction. *Surf. Sci.* **2000**, *454−456*, 316−319.
(15) Kratzer, P.; Brenig, W. Highly excited molecules from Eley-Rideal reactions. *Surf. Sci.* **1991**, *254*, 275−280.

DOI: 10.1021/jp511847w
J. Phys. Chem. C 2015, 119, 3171−3179

(16) Jackson, B.; Persson, M. Vibrational excitation in recombinative desorption of hydrogen on metal surfaces: Eley-Rideal mechanism. *Surf. Sci.* **1991**, *269*, 195−200.
(17) Jackson, B.; Persson, M. A quantum mechanical study of recombinative desorption of atomic hydrogen on a metal surface. *J. Chem. Phys.* **1992**, *96*, 2378−2387.
(18) Shin, H. K. Vibrationally excited molecules from the reaction of H atoms and chemisorbed H atoms on a metal surface. *Chem. Phys. Lett.* **1995**, *244*, 235−244.
(19) Persson, M.; Jackson, B. Isotope effects in the Eley-Rideal dynamics of the recombinative desorption of hydrogen on a metal surface. *Chem. Phys. Lett.* **1995**, *237*, 468−473.
(20) Caratzoulas, S.; Jackson, B.; Persson, M. Eley-Rideal and hot-atom reaction dynamics of H(g) with H adsorbed on Cu(111). *J. Chem. Phys.* **1997**, *107*, 6420−6431.
(21) Shalashilin, D. V.; Jackson, B.; Persson, M. Eley-Rideal and hot-atom dynamics of HD formation by H(D) incident from the gas phase on D(H)-covered Cu(111). *Faraday Discuss.* **1998**, *110*, 287−300.
(22) Shalashilin, D. V.; Jackson, B.; Persson, M. Eley-Rideal and hot-atom reactions of H(D) atoms with D(H)-covered Cu(111) surfaces: quasiclassical studies. *J. Chem. Phys.* **1999**, *110*, 11038−11046.
(23) Kalyanaraman, C.; Lemoine, D.; Jackson, B. Eley-Rideal and hot-atom reactions between hydrogen atoms on metals: quantum mechanical studies. *Phys. Chem. Chem. Phys.* **1999**, *1*, 1351−1358.
(24) Jackson, B.; Lemoine, D. Eley-Rideal reactions between H atoms on metal and graphite surfaces: The variation of reactivity with substrate. *J. Chem. Phys.* **2001**, *114*, 474−482.
(25) Guvenc, Z. B.; Sha, X.; Jackson, B. Eley-Rideal and hot atom reactions between hydrogen atoms on Ni(100): Electronic structure and quasiclassical studies. *J. Chem. Phys.* **2001**, *115*, 9018−9027.
(26) Lemoine, D.; Quattrucci, J. D.; Jackson, B. Efficient Eley-Rideal Reactions of H Atoms with Single Cl Adsorbates on Au(111). *Phys. Rev. Lett.* **2002**, *89*, 268302.
(27) Jackson, B.; Sha, X.; Guvenc, Z. B. Kinetic model for Eley-Rideal and hot atom reactions between H atoms on metal surfaces. *J. Chem. Phys.* **2002**, *116*, 2599−2608.
(28) Guvenc, Z. B.; Sha, X.; Jackson, B. The Effects of Lattice Motion on Eley-Rideal and Hot Atom Reactions: Quasiclassical Studies of Hydrogen Recombination on Ni(100). *J. Phys. Chem. B* **2002**, *106*, 8342−8348.
(29) Quattrucci, J. G.; Jackson, B.; Lemoine, D. Eley−Rideal reactions of H atoms with Cl adsorbed on Au(111): Quantum and quasiclassical studies. *J. Chem. Phys.* **2003**, *118*, 2357−2365.
(30) Martinazzo, R.; Assoni, S.; Marinoni, G.; Tantardini, G. F. Hot-atom versus Eley−Rideal dynamics in hydrogen recombination on Ni(100). I. The single-adsorbate case. *J. Chem. Phys.* **2004**, *120*, 8761−8771.
(31) Lanzani, G.; Martinazzo, R.; Materzanini, G.; Pino, I.; Tantardini, G. F. Chemistry at surfaces: from *ab initio* structures to quantum dynamics. *Theor. Chem. Acc.* **2007**, *117*, 805−825.
(32) Rutigliano, M.; Cacciatore, M. Eley-Rideal recombination of hydrogen atoms on a tungsten surface. *Phys. Chem. Chem. Phys.* **2011**, *13*, 7475−7484.
(33) Blanco-Rey, M.; Diaz, E.; Bocan, G. A.; Muino, R. D.; Alducin, M.; Juaristi, J. I. Efficient N_2 Formation on Ag(111) by Eley-Rideal Recombination of Hyperthermal Atoms. *J. Phys. Chem. Lett.* **2013**, *4*, 3704−3709.
(34) Langmuir, I. Heterogeneous reactions, chemical reactions on surfaces. *Trans. Faraday Soc.* **1922**, *17*, 607.
(35) Harris, J.; Kasemo, B. On precursor mechanisms for surface reactions. *Surf. Sci.* **1981**, *105*, L281−L287.
(36) Strömquist, J.; Bengtsson, L.; Persson, M.; Hammer, B. The dynamics of H absorption in and adsorption on Cu(111). *Surf. Sci.* **1998**, *397*, 382−394.
(37) Blanco-Rey, M.; Juaristi, J.; Muiño, R. D.; Busnengo, H.; Kroes, G.; Alducin, M. Electronic Friction Dominates Hydrogen Hot-Atom Relaxation on Pd (100). *Phys. Rev. Lett.* **2014**, *112*, 103203.
(38) Persson, M.; Jackson, B. Flat surface study of the Eley-Rideal dynamics of recombinative desorption of hydrogen on a metal surface. *J. Chem. Phys.* **1995**, *102*, 1078−1093.
(39) Jackson, B.; Persson, M. Effects of isotopic substitution on Eley-Rideal reactions and adsorbate-mediated trapping. *J. Chem. Phys.* **1995**, *103*, 6257−6279.
(40) Guvenc, Z. B.; Guvenc, D. Hydrogen recombination on a mixed adsorption layer at saturation on a metal surface: H → $(D+H)_{sat}$ + Ni(100). *Surf. Sci.* **2003**, *529*, 11−22.
(41) Vurdu, C. D.; Ozcelik, S.; Guvenc, Z. B. Quasiclassical study of Eley-Rideal and hot-atom reactions on a surface at 94K: H(D) -> D(H) + Cu(111). *Surf. Sci.* **2007**, *601*, 3745.
(42) Vurdu, C. D.; Guvenc, Z. B. H(D) D(H) + Cu(111) collision system: Molecular dynamics study of surface temperature effects. *J. Chem. Phys.* **2011**, *134*, 164306.
(43) Kleyn, A. W.; Cardozo, N. J. L.; Samm, U. Plasma-surface interaction in the context of ITER. *Phys. Chem. Chem. Phys.* **2006**, *8*, 1761−1774.
(44) Barabash, V.; Federici, G.; Matera, R.; Raffray, A. R.; Teams, I. H. Armour Materials for the ITER Plasma FAcing Components. *Phys. Scr.* **1999**, *T81*, 74−83.
(45) Federici, G.; Wuerz, H.; Janeschitz, G.; Tivey, R. Erosion of plasma-facing components in ITER. *Fusion Eng. Des.* **2002**, *61*−*62*, 81−94.
(46) Federici, G.; Andrew, P.; Barabaschi, P.; Brooks, J.; Doerner, R.; Geier, A.; Herrmann, A. Key ITER plasma edge and plasma−material interaction issues. *J. Nucl. Mater.* **2003**, *313*, 11−22.
(47) Roth, J.; Tsitrone, E.; Loarte, A.; Loarer, T.; Counsell, G.; Neu, R.; Philipps, V.; Brezinsek, S.; Lehnen, M.; Coad, P.; et al. Recent analysis of key plasma wall interactions issues for {ITER}. *J. Nucl. Mater.* **2009**, *390*−*391*, 1−9.
(48) Pétuya, R.; Larregaray, P.; Crespos, C.; Busnengo, H. F.; Martinez, A. E. Dynamics of H_2 Eley-Rideal abstraction from W(110): Sensitivity to the representation of the molecule-surface potential. *J. Chem. Phys. 141*, 024701.
(49) Pétuya, R.; Crespos, C.; Quintas-Sánchez, E.; Larrégaray, P. Comparative Theoretical Study of H_2 Eley-Rideal Recombination Dynamics on W(100) and W(110). *J. Phys. Chem. C* **2014**, *118*, 11704−11710.
(50) Chung, J. W.; Ying, S. C.; Estrup, P. J. Reconstruction of the W(110) Surface Induced by Hydrogen Adsorption. *Phys. Rev. Lett.* **1986**, *56*, 749−752.
(51) Gonchar, V. V.; Kanash, O. V.; Naumovets, A. G.; Fedorus, A. G. Two-dimensional lattices of adsorbed hydrogen on the (011) face of tungsten and their disordering. *JETP Lett.* **1978**, *28*, 330−333.
(52) Lyuksyutov, I. F.; Fedorus, A. G. Critical exponents of the H-W(001) system. *Sov. Phys. JETP* **1981**, *53*, 1317−1321.
(53) Gonchar, V. V.; Kagan, Y. M.; Kanash, O. V.; Naumovets, A. G.; Fedorus, A. G. Two-dimensional hydrogen and deuterium lattices on the (011) face of tungsten and their thermal and electron-stimulated disordering. *Sov. Phys. JETP* **1983**, *57*, 142−148.
(54) Balden, M.; Lehwald, S.; Ibach, H.; Mills, D. L. Hydrogen Coverred W(110) Surface: A Hydrogen Liquid with a Propensity for One-Dimensional Order. *Phys. Rev. Lett.* **1994**, *73*, 854−857.
(55) Balden, M.; Lehwald, S.; Ibach, H. Substrate and hydrogen phonons of the ordered *p* (2×1) and (2×2) phase and the anomalous (1×1) phase of hydrogen on W(110). *Phys. Rev. B* **1996**, *53*, 7479−7491.
(56) Arnold, M.; Hupfauer, G.; Bayer, P.; Hammer, L.; Heinz, K.; Kohler, B.; Scheffler, M. Hydrogen on W(110): an adsorption structure revisited. *Surf. Sci.* **1997**, *382*, 288−299.
(57) Wang, S. C.; Gomer, R. Diffusion of hydrogen, deuterium, and tritium on the (110) plane of tungsten. *J. Chem. Phys.* **1985**, *83*, 4193−4209.
(58) Bungaro, C.; de Gironcoli, S.; Baroni, S. Theory of the Anomalous Rayleigh Dispersion at H/W(110) Surfaces. *Phys. Rev. Lett.* **1996**, *77*, 2491−2494.

DOI: 10.1021/jp511847w
J. Phys. Chem. C 2015, 119, 3171−3179

(59) Nojima, A.; Yamashita, K. A theoretical study of hydrogen adsorption and diffusion on a W(110) surface. *Surf. Sci.* **2007**, *601*, 3003−3011.
(60) Busnengo, H. F.; Salin, A.; Dong, W. Representation of the 6D potential energy surface for a diatomic molecule near a solid surface. *J. Chem. Phys.* **2000**, *112*, 7641−7651.
(61) Busnengo, H. F.; Martinez, A. E. H_2 Chemisorption on W(100) and W(110) Surfaces. *J. Phys. Chem. C* **2008**, *112*, 5579−5588.
(62) Kwak, K. W.; Chou, M. Y.; Troullier, N. First-principles study of the H-induced reconstruction of W(110). *Phys. Rev. B* **1996**, *53*, 13734−13738.
(63) Schofield, P. Computer simulation studies of the liquid state. *Comput. Phys. Commun.* **1973**, *5*, 17−23.
(64) Beeman, D. Some multistep methods for use in molecular dynamics calculations. *J. Comput. Phys.* **1976**, *20*, 130−139.
(65) Bonnet, L.; Rayez, J. C. Quasiclassical trajectory method for molecular scattering processes: necessity of a weighted binning approach. *Chem. Phys. Lett.* **1997**, *277*, 183−190.
(66) Bonnet, L.; Rayez, J. C. Gaussian weighting in the quasiclassical trajectory method. *Chem. Phys. Lett.* **2004**, *397*, 106−109.
(67) Espinosa-Garcia, J.; Bonnet, L.; Corchado, J. C. Classical description in a quantum spirit of the prototype four-atom reaction OH + D_2. *Phys. Chem. Chem. Phys.* **2010**, *12*, 3873−3877.
(68) Quintas-Sánchez, E.; Larrégaray, P.; Crespos, C.; Martin-Gondre, L.; Rubayo-Soneira, J.; Rayez, J.-C. Dynamical reaction pathways in Eley-Rideal recombination of nitrogen from W(100). *J. Chem. Phys.* **2012**, *137*, 064709.
(69) Quintas-Sánchez, E.; Crespos, C.; Rayez, J.-C.; Martin-Gondre, L.; Rubayo-Soneira, J. Surface temperature effects on the dynamics of N_2 Eley-Rideal recombination on W(100). *J. Chem. Phys.* **2013**, *138*, 024706.
(70) Markelj, S.; Cadez, I. Production of vibrationally excited hydrogen molecules by atom recombination on Cu W materials. *J. Chem. Phys.* **2011**, *134*, 124707.
(71) Ramos, M.; Minniti, M.; Díaz, C.; Miranda, R.; Martin, F.; Martinez, A. E.; Busnengo, H. F. Environment-driven reactivity of H_2 on Pd Ru surface alloys. *Phys. Chem. Chem. Phys.* **2013**, *15*, 14936−14940.

DOI: 10.1021/jp511847w
J. Phys. Chem. C 2015, 119, 3171−3179